

OPTIMAL MODEL SWITCHING FOR GAS FLOW IN PIPE NETWORKS

FABIAN RÜFFLER¹, VOLKER MEHRMANN², FALK M. HANTE¹

ABSTRACT. We consider model adaptivity for gas flow in pipeline networks. For each instant in time and for each pipe in the network a model for the gas flow is to be selected from a hierarchy of models in order to maximize a performance index that balances model accuracy and computational cost for a simulation of the entire network. This combinatorial problem involving partial differential equations is posed as an optimal switching control problem for abstract semilinear evolutions. We provide a theoretical and numerical framework for solving this problem using a two stage gradient descent approach based on switching time and mode insertion gradients. A numerical study demonstrates the practicability of the approach.

Keywords. Gas Networks, Model Adaptivity, Switching Systems, Strongly Continuous Semigroups, Optimization

1. INTRODUCTION

Modeling, simulation and optimization of critical infrastructure systems such as traffic, electricity, water or natural gas networks play an increasingly important role in our society. Many of these problems involve aspects of dynamic energy transportation and distribution in networks. The optimization with respect to efficiency, robustness, or environmental performance requires the use of high-resolution dynamical models in form of time-dependent differential equations. As a particular case, we consider transportation and distribution of natural gas in a network of pipelines, where the high-resolution models refer to the one-dimensional Euler gas equations coupled with further dynamics representing active or passive network elements such as compressors, resistors and control valves.

Detailed models for gas flow in pipeline networks are well established, see e.g., [3, 7, 12]. Similar maturity has been achieved for time-simulation methods, see e.g., [1, 10, 20], the analysis of stationary states [14], the time-continuous optimal control of compressors using adjoint techniques [17, 26], and feedback stabilization based on classical solutions [9]. If the discrete nature of control valves being open or closed is to be taken into account, then the optimization needs to deal with mixed integer and continuous type variables simultaneously. Similar decisions are often to be taken into account also in other critical infrastructure systems.

In industrial practice the treatment of switched systems is often carried out by first applying a full space-time discretization of the systems and then using a mixed-integer nonlinear programming tool that incorporates the switches as extra variables to be optimized, see e.g., [5, 4, 32]. Another approach is to restrict the optimization to the stationary case where special purpose techniques can be successfully applied [29]. A temporal expansion of these techniques on a full network currently seems to be out of scope, see, e.g., [15, 25]. We proceed in yet another way via a *model switching approach*, see [16]. Since networks already provide a natural spatial partition by the edges representing pipes, it seems natural to minimize a global model error by selecting either one of several models in a dynamic model hierarchy [11, 10] or a stationary model hierarchy

¹Friedrich-Alexander-Universität Erlangen-Nürnberg (FAU), Lehrstuhl Angewandte Mathematik II, Cauerstr. 11, 91058 Erlangen, Germany (fabian.rueffler@fau.de and falk.hante@fau.de); ² Technische Universität Berlin, Straße des 17. Juni 136, 10623 Berlin, Germany (mehrmann@math.tu-berlin.de).

[26] for each pipe as a function of time. To do this, it is important to identify regions in the time expanded network problem where stationary models still provide a reasonable approximation in the sense that the global error remains small. A particular difficulty that the model switching problem for gas networks has in common with most of the other mentioned applications is the high-resolution model being a partial differential equation (typically a system of balance laws). While the computation of optimal switching for ordinary differential equations and differential-algebraic equations is theoretically and numerically well studied, see [8, 13, 18, 19, 24, 27, 34, 35, 36, 37], the corresponding theory involving certain types of partial differential equations is still under development [30, 31].

Our main contribution in this paper is to provide a theoretical and numerical framework for solving the model switching problem using the example of gas networks. We show that the problem can be casted in the sense of switching among a family of abstract evolution equations on an appropriate Banach space. This allows us to use adjoint based gradient representations for switching time and mode sequence variations recently developed in [30] to characterize locally optimal solutions for the model switching problem by introducing the notion of first order stationarity. This, in turn, motivates a two stage gradient decent approach conceptually introduced and analyzed in [2] for the optimization of switching sequences in the context of ordinary differential equations for numerical solutions of the model switching problem. We provide results for a proof-of-concept implementation for a gas network comprising 340 km of pipes on a 30 min time horizon.

The paper is organized as follows. In Section 2 we provide a more detailed description of the common gas network models. In particular, we briefly discuss a semilinear simplification of the Euler gas equations as the most detailed model on a pipe and consider the corresponding stationary solutions. Moreover, we introduce the model switching problem. In Section 3, we show that the equations on a network coupling these models for the pipes along with appropriate coupling conditions on the nodes allowing further network elements such as valves and compressors is well-posed in the sense of being equivalently represented by a nonlinear perturbation of a strongly continuous semigroup in a suitable Sobolev space. In Section 4 we apply the well-posedness result to define an appropriate system of adjoint equations and to derive a stationarity concept based on switching-time gradients and mode-insertion gradients as a first order optimality condition for model optimality. Further, we present details of a conceptual algorithm alternating between switching-time optimization and mode-insertion in order to compute a solution of the model switching problem in the sense of our stationarity concept. In Section 5 we present a numerical study. In Section 6 we discuss applications and directions of future work.

2. GAS NETWORK MODELING

2.1. A model hierarchy for single pipes. The one-dimensional isothermal Euler equations are given by a system of nonlinear hyperbolic partial differential equations (PDEs), which describe the motion of a compressible non-viscous gas in long high-pressure pipelines. They consist of the continuity equation and the balance of moments (see, e.g., [33, 6, 23, 22])

$$(1) \quad \begin{aligned} \partial_t \varrho + \partial_x(\varrho v) &= 0, \\ \partial_t(\varrho v) + \partial_x(P + \varrho v^2) &= -\theta \varrho v |v| - g \varrho h', \end{aligned}$$

where ϱ denotes the density in $\frac{\text{kg}}{\text{m}^3}$, v the velocity in $\frac{\text{m}}{\text{s}}$, P the pressure of the gas in $\frac{\text{kg}}{\text{m s}^2}$, g the gravitational constant and h' the slope of the pipe. Furthermore $\theta = \frac{\lambda}{2D}$, where λ is the friction coefficient of the pipe, and D is the diameter of the pipe. The conserved, respectively balanced, quantities of the system are the density ϱ and the flux $q = \varrho v$. In addition to system (1) we use

the constitutive law for a real gas

$$P = R_s \varrho T_0 Z(P, T_0),$$

where $Z(P, T_0)$ is the gas compressibility factor at constant temperature T_0 and R_s is the specific gas constant. For an ideal gas one has $Z(P) \equiv 1$.

For convenience, we assume small velocities $|v| \ll c$ and a constant gas compressibility factor $Z(P, T_0) \equiv \bar{Z}$. This yields a constant speed of sound $c = \sqrt{P/\varrho}$. For natural gas, indeed one typically has $|v| \leq 5 \frac{\text{m}}{\text{s}}$ and $c \approx 340 \frac{\text{m}}{\text{s}}$. Under such conditions, we have $P + \varrho v^2 = P(1 + \frac{v^2}{c^2}) \approx 1$ and System (1) becomes

$$(2) \quad \begin{aligned} \partial_t \varrho + \partial_x q &= 0, \\ \partial_t q + c^2 \partial_x \varrho &= -\theta \frac{q|q|}{\varrho} - gh' \varrho. \end{aligned}$$

This model exhibits two simple characteristics $\lambda_1 = -c$ and $\lambda_2 = c$.

Assuming the solution to be stationary, i.e. $\partial_t \varrho = \partial_t q = 0$, we arrive at the model

$$(3) \quad \begin{aligned} \partial_x q &= 0, \\ \partial_x \varrho &= -\theta \frac{q|q|}{\varrho} - gh' \varrho. \end{aligned}$$

Here, the flux q is constant in space and time $q(t, x) = \bar{q}$ and $\varrho(t, x) = \bar{\varrho}(x)$ with $\bar{\varrho}$ being a solution of the momentum equation in (3), which is a Bernoulli-equation. A solution of the momentum equation can therefore be obtained algebraically, for example, for horizontal pipes we have $h' = 0$ and obtain

$$(4) \quad \bar{\varrho}(x) = \sqrt{\varrho(0)^2 - \frac{2\theta x}{c^2} q|q|}.$$

A similar model hierarchy can also be considered for the case of non-isothermal flow, see e.g., [12], and analogously also for the case of similar infrastructure systems such as water distribution networks [16].

2.2. Networks with pipes, valves, and compressors. For $m, n \in \mathbb{N}$ we consider a network of pipes that we model by a metric graph $G = (V, E)$ with nodes $V = (v_1, \dots, v_m)$ and edges $E = (e_1, \dots, e_n) \subseteq V \times V$. For each edge $e \in E$, call $e(1)$ the *left node* and $e(2)$ the *right node* of e . We demand the incident nodes of every edge to be different, so $e(1) \neq e(2)$ for any $e \in E$ and thus *self-loops* are not allowed. On the other hand, if $v \in V$ is any node, then we define

$$\begin{aligned} \text{the set of ingoing edges by } \delta^+ v &= \{e \in E \mid e(2) = v\}, \\ \text{the set of outgoing edges by } \delta^- v &= \{e \in E \mid e(1) = v\}, \\ \text{the set of incident edges by } \delta v &= \delta^- v \cup \delta^+ v. \end{aligned}$$

The number $|\delta v|$ then is called the *degree* of node $v \in V$.

With each edge $e_j \in E$ of such a network, we associate a pipe model from the hierarchy in Section 2.1 and a given pipe length $L^j > 0$. Furthermore, depending on the role of each node in the network, we impose appropriate coupling conditions for the gas density and flow at the boundary of pipes corresponding to edges being incident to that node. To this end, we define for $v \in V$ and $e_j \in \delta v$

$$x(v, e_j) = \begin{cases} 0, & \text{if } e_j \in \delta^- v, \\ 1, & \text{if } e_j \in \delta^+ v. \end{cases}$$

For each node $v \in V$, we then impose a transmission condition for the density and a balance equation for the fluxes at the node. The transmission condition states that the density variables ϱ^j

weighted by given factors $\alpha \in (0, \infty)^{m \times 2}$ coincide for all incident edges $e \in \delta v$ and can be expressed as

$$\alpha_{x(v, e_k)}^k \varrho^k(t, L_k x(v, e_k)) = \alpha_{x(v, e_l)}^l \varrho^l(t, L_l x(v, e_l)), \quad \forall e_k, e_l \in \delta v, t \in [0, T].$$

The nodal balance equation for a given outflow function $q^v : [0, T] \rightarrow \mathbb{R}$ is similar to a classical Kirchhoff condition for the fluxes q^j and can be written as

$$\sum_{e_j \in \delta^+ v} q^j(t, L_j) - \sum_{e_j \in \delta^- v} q^j(t, 0) = q^v(t), \quad t \in [0, T].$$

The choice of α corresponds to the nodal types in the network. Prototypically, we will consider the following cases:

Junctions: nodes v such that $q^v \equiv 0$ and $\alpha_{x(v, e_k)}^k = 1$ for all $e_k \in \delta v$.

Boundary nodes: nodes v such that $\alpha_{x(v, e_k)}^k = 1$ for all $e_k \in \delta v$, but $q^v \not\equiv 0$. We also refer to v as an *entry node*, if $q^v < 0$, or an *exit node*, if $q^v > 0$.

Compressors: nodes v with $q^v \equiv 0$ and $|\delta^+ v| = |\delta^- v| = 1$. A description established via the characteristic diagram based on measured specific changes in adiabatic enthalpy H_{ad} of the compression process yields the model

$$H_{\text{ad}} = \bar{Z} T_0 R_s \frac{\kappa}{\kappa - 1} \left(\left(\frac{\varrho^l(0, t)}{\varrho^k(L_k, t)} \right)^{\frac{\kappa-1}{\kappa}} - 1 \right), \quad e_k \in \delta^+ v, e_l \in \delta^- v, t \in [0, T],$$

where κ is a compressor specific constant, \bar{Z} is the gas compressibility factor that is assumed to be constant and H_{ad} is within flow dependent and compressor specific bounds obtained from the characteristic diagram. In consistency with the pipe models, we assume that H_{ad} is given by a known reference \bar{H}_{ad} . Then we get

$$\varrho^l(0, t) = \bar{\alpha} \varrho^k(L_k, t), \quad e_k \in \delta^+ v, e_l \in \delta^- v, t \in [0, T]$$

with a compressor specific factor

$$(5) \quad \bar{\alpha} = \left(1 + \frac{(\kappa - 1) \bar{H}_{\text{ad}}}{\kappa \bar{Z} T_0 R_s} \right)^{\frac{\kappa}{\kappa - 1}}.$$

This yields $\alpha_1^k = 1$ and $\alpha_0^l = \bar{\alpha}$.

We note that gas networks typically involve further network components such as valves, resistors, gas coolers, etc. For appropriate coupling conditions we refer to [29].

2.3. The model switching problem. We now discuss switching between the two models (2) and (3) in order to efficiently resolve the dynamics of the gas flow in a network. The idea is that, with the exception of locally high fluctuation, in realistic scenarios the solution to (2) is on big parts of the network close to the stationary model (3). In these regions we thus can freeze the solution with an acceptable loss in accuracy to save computational effort. By comparison with the solution fully simulated with (2) we then can set up a cost functional measuring the deviation of the partially frozen solution in some appropriate norm. Adding a performance function measuring the time steps where the costly model (2) is calculated, we can set up the optimization problem of weighting the accuracy against the computational effort. Solving this problem enables us to identify a time-dependent model selection for the simulation of gas dynamics on networks that can be used in further examinations to get a cheaply solvable system.

More precisely, we can introduce the model

$$(6) \quad \begin{aligned} \varepsilon \partial_t \varrho + \partial_x q &= 0, \\ \varepsilon \partial_t q + c^2 \partial_x \varrho &= -\theta \frac{q|q|}{\varrho} - gh' \varrho \end{aligned}$$

for fixed $c, \theta > 0$, which agrees with (2) in the case $\varepsilon = 1$ while (3) corresponds to the limit case $\varepsilon \searrow 0$. In order to avoid technical problems with the coupling conditions of the two different models on networks, in the following we consider switching the parameter ε between 1 and a positive value $\bar{\varepsilon} > 0$ close to zero. This is justified theoretically, since the solution of (6) depends continuously on ε and thus is close to that of (3) for sufficiently small ε . On the other hand, this allows us to still use (3) in the numerical realisation as adequate but cheap replacement of the fine model.

Let $G = (V, E)$ be a network, where the type of each node $v \in V$ is given by the parameters α and q^v as in Section 2.2. On each edge e_j of length L_j we have an initial gas density ϱ_0^j and gas flow q_0^j . For any finite sequence of modes $\mu = (\mu_k)_{k=1, \dots, N} \subseteq \{0, 1\}^n$, representing the choice for ε in (6), and any monotonically increasing sequence of switching times $\tau = (\tau_k)_{k=0, \dots, N+1} \subseteq [0, \infty)$ consider the PDE-system

$$(7) \quad \begin{aligned} \varepsilon_{\mu_k(j)} \partial_t \varrho^j(t, x) + \partial_x q^j(t, x) &= 0, \\ \varepsilon_{\mu_k(j)} \partial_t q^j(t, x) + c^2 \partial_x \varrho^j(t, x) &= -\theta \frac{q^j(t, x) |q^j(t, x)|}{\varrho^j(t, x)} - gh' \varrho^j(t, x), \end{aligned}$$

where $x \in [0, L_j]$ for $j = 1, \dots, n$ and $t \in (\tau_{k-1}, \tau_k)$ for $k = 1, \dots, N$. Here,

$$\varepsilon_{\mu_k(j)} = \begin{cases} \bar{\varepsilon}, & \text{if } \mu_k(j) = 0, \\ 1, & \text{if } \mu_k(j) = 1 \end{cases}$$

and $\varrho^j(0, x) = \varrho_0^j(x)$, $q^j(0, x) = q_0^j(x)$ for $x \in [0, L_j]$ and given initial states ϱ_0^j, q_0^j . Moreover, at any time point $t \in [\tau_0, \tau_N]$, density and flux additionally satisfy the node coupling conditions

$$(8) \quad \begin{aligned} \alpha_{x(v, e_i)}^i \varrho^i(t, L_i x(v, e_i)) &= \alpha_{x(v, e_j)}^j \varrho^j(t, L_j x(v, e_j)), \quad \forall e_i, e_j \in \delta v, \\ \sum_{e_j \in \delta^+ v} q^j(t, L_j) - \sum_{e_j \in \delta^- v} q^j(t, 0) &= q^v(t) \end{aligned}$$

for each $v \in V$, explained in Section 2.2.

Denote by $z_d = ((\varrho_d^j)_j, (q_d^j)_j)$ the reference solution to (7),(8) for the choice $N = 1$, $\mu = 1$ and $\tau = (0, T)$, which corresponds to the fine model (2) being fully solved on the complete network and the existence of which will be proven in Section 3. For any other $z = ((\varrho^j)_j, (q^j)_j)$ then define the cost functional

$$(9) \quad \begin{aligned} J(\mu, \tau, z) &= \sum_{j=1}^n \int_0^T \int_0^{L_j} \gamma_1 (\varrho^j(t, x) - \varrho_d^j(t, x))^2 + \gamma_2 (q^j(t, x) - q_d^j(t, x))^2 dx dt \\ &+ \gamma_3 \sum_{k=1}^N \sum_{j=1}^n \frac{1}{L_j} \int_{\tau_k}^{\tau_{k+1}} (\mu_k(m) - \bar{\varepsilon})^2 dt, \\ &+ \gamma_4 N \end{aligned}$$

with $\gamma_1, \dots, \gamma_4 \geq 0$, where the first term measures the deviation of z from z_d , the second term penalizes using the fine model (2) and the third term penalizes the number of switching time

points. Note that, since longer pipes mean more computational effort when using the fine model, the lengths L_j of the pipes enter into the cost as well. For later reference, we set

$$(10) \quad \begin{aligned} l(t, z) &= \sum_{j=1}^n \int_0^{L_j} (\varrho^j(t, x) - \varrho_d^j(t, x))^2 + \frac{1}{c^2} (q^j(t, x) - q_d^j(t, x))^2 dx, \\ J_1 &= \frac{\gamma_1}{2} \int_0^T l(t, z) dt, \\ J_2 &= \gamma_2 \sum_{k=1}^N \sum_{j=1}^n \frac{1}{L_j} \int_{\tau_k}^{\tau_{k+1}} (\mu_k(m) - \bar{\varepsilon})^2 dt + \gamma_3 N, \end{aligned}$$

then $J = J_1 + J_2$.

The challenge now is to choose the sequences μ and τ such that, with z being the corresponding solution to (7),(8), the cost functional J is minimized. Hence our objective is to solve the minimization problem

$$(11) \quad \begin{aligned} \min_{(\mu, \tau)} \quad & J(\mu, \tau, z) \\ \text{s.t.} \quad & z \text{ solves (7), (8) for the switching sequence } (\mu, \tau). \end{aligned}$$

3. SEMIGROUP FORMULATION ON NETWORKS

In this section, we will set up an abstract formulation of the PDE-system in (7) for $\tau = (0, T)$ and any fixed choice of modes per edge and prove a result about the existence and uniqueness of a classical solution. By induction, this will yield well-posedness of (7) for any finite switching sequence. For each $j \in \{1, \dots, n\}$, we now consider the initial boundary value problem for $z^j = (\varrho^j, q^j)^\top$ on pipe $e_j \in E$ given by

$$(12) \quad \begin{aligned} z_t^j(t, x) + A^j z_x^j(t, x) &= f^j(z^j(t, x)), \quad t \in [0, T], x \in [0, L_j], \\ z^j(0, x) &= z_0^j(x), \quad x \in [0, L_j], \end{aligned}$$

and the coupling conditions

$$(13) \quad \alpha_{x(v, e_k)}^k z_1^k(t, L_k x(v, e_k)) = \alpha_{x(v, e_l)}^l z_1^l(t, L_l x(v, e_l)) \quad \forall e_k, e_l \in \delta v,$$

$$(14) \quad \sum_{e_j \in \delta^+ v} z_2^j(t, L_j) - \sum_{e_j \in \delta^- v} z_2^j(t, 0) = q_0^v(t)$$

for each node $v \in V$. Here, $L_j > 0$, $z_0^j: [0, L_j] \rightarrow \mathbb{R}^2$, $f^j \in C^1(\mathbb{R}^2, \mathbb{R}^2)$ is globally Lipschitz-continuous and

$$A^j = \frac{1}{\varepsilon_j} \begin{bmatrix} 0 & 1 \\ c_j^2 & 0 \end{bmatrix} \quad \text{for some } \varepsilon_j, c_j > 0$$

for each $j \in \{1, \dots, n\}$. Moreover, $\alpha \in (0, \infty)^{m \times 2}$ and $q_0^v: [0, \infty) \rightarrow \mathbb{R}$ is a given outflow for each $v \in V$. Introduce the space

$$Z = \left[\bigotimes_{j=1}^n L^2([0, L_j], \mathbb{R}^2) \right] \otimes L^2([0, \infty), \mathbb{R}^m),$$

the vectors

$$\begin{aligned} z &= ((z^1)^\top, \dots, (z^n)^\top, q^{v_1}, \dots, q^{v_m})^\top, \\ z_0 &= ((z_0^1)^\top, \dots, (z_0^n)^\top, q_0^{v_1}, \dots, q_0^{v_m})^\top \end{aligned}$$

the operators

$$(15) \quad A = \begin{bmatrix} A^1 & & \\ & \ddots & \\ & & A^n \end{bmatrix} \frac{\partial}{\partial x}, \quad B = -\mathbf{1}_m \frac{\partial}{\partial x} \quad \text{and}$$

$$f(z) = (f^1(z^1), \dots, f^n(z^n), 0, \dots, 0)^\top.$$

Moreover, define the operator $\text{diag}(A, B)$ on the domain

$$(16) \quad D \left(\begin{bmatrix} A & 0 \\ 0 & B \end{bmatrix} \right) = \left\{ z = (z^1, \dots, z^n, q^{v_1}, \dots, q^{v_m})^\top \in Z \mid z \text{ is absolutely continuous,} \right.$$

$$\alpha_{x(v, e_k)}^k z_1^k(L_k x(v, e_k)) = \alpha_{x(v, e_l)}^l z_1^l(L_l x(v, e_l)) \quad \forall v \in V, e_k, e_l \in \delta v,$$

$$\left. \sum_{e_j \in \delta^+ v} z_2^j(L_j) - \sum_{e_j \in \delta^- v} z_2^j(0) = q^v(0) \quad \forall v \in V \right\}$$

of all vectors of absolutely continuous functions that satisfy the boundary conditions (13) and (14). Note that, though the inflow functions q^v is only evaluated at the origin, it also is shifted in time due to the transport-type evolution represented by operator B – this together enforces the originally time-dependent coupling condition (14). We then can reformulate system (12)-(14) as the abstract initial-value problem

$$(17) \quad \dot{z}(t) + \begin{bmatrix} A & 0 \\ 0 & B \end{bmatrix} z(t) = f(z), \quad t \in [0, T],$$

$$z(0) = z_0.$$

Now we can state the following result:

Theorem 3.1. *The operator*

$$\left(D \left(\begin{bmatrix} A & 0 \\ 0 & B \end{bmatrix} \right), \begin{bmatrix} A & 0 \\ 0 & B \end{bmatrix} \right)$$

is the infinitesimal generator of a strongly continuous semigroup on Z .

Proof. Note that $\text{diag}(A, B)$ is a densely defined, closed operator on Z with a nonempty resolvent set (for instance $0 \in \rho(\text{diag}(A, B))$). Following [28, Chapter 4, Theorem 1.3], to prove the claimed semigroup property, it thus suffices to show that the homogeneous system

$$(18) \quad \dot{z}(t) + \begin{bmatrix} A & 0 \\ 0 & B \end{bmatrix} z(t) = 0, \quad t \in [0, T],$$

$$z(0) = z_0.$$

has a unique solution $z \in C^1([0, T], Z)$ for any $T > 0$ and every choice $z_0 \in D(\text{diag}(A, B))$. So let

$$z_0 = (\varrho_0^1, q_0^1, \dots, \varrho_0^n, q_0^n, q_0^{v_1}, \dots, q_0^{v_m})^\top \in D(\text{diag}(A, B))$$

be given and first assume $T \leq \bar{T} := \min \left\{ \frac{\varepsilon_j L_j}{2c_j} \mid j = 1, \dots, n \right\} > 0$. We recognise in the operator B a transport equation with velocity -1 for the variables q^{v_1}, \dots, q^{v_m} with the well-known unique solution

$$q^{v_k}(t, s) = q_0^{v_k}(s + t).$$

Next, for each note $v \in V$ we can set

$$\alpha_v = \left(\sum_{e_j \in \delta^+ v} \alpha_1^j c_j + \sum_{e_j \in \delta^- v} \alpha_0^j c_j \right) > 0$$

and

$$\begin{aligned} \varrho^v(t) = \alpha_v^{-1} & \left[\sum_{e_j \in \delta^+ v} \left(c_j \varrho_0^j \left(L_j - \frac{c_j}{\varepsilon_j} t \right) + q_0^j \left(L_j - \frac{c_j}{\varepsilon_j} t \right) \right) \right. \\ & \left. + \sum_{e_j \in \delta^- v} \left(c_j \varrho_0^j \left(\frac{c_j}{\varepsilon_j} t \right) - q_0^j \left(\frac{c_j}{\varepsilon_j} t \right) \right) + q^v(t, 0) \right]. \end{aligned}$$

Since $\varrho^1, q^1, \dots, \varrho^n, q^n, q^{v_1}, \dots, q^{v_m}$ are absolutely continuous, so is ϱ^v for each $v \in V$. For each edge $e_j \in E$, $j = 1, \dots, n$, construct the functions $\varrho^j, q^j: [0, T] \times [0, 1] \rightarrow \mathbb{R}$ as follows: for $t \in (0, T]$ set

$$\begin{aligned} \varrho^j(t, 0) &= \alpha_0^j \varrho^{e_j(1)}(t), \quad q^j(t, 0) = -\alpha_0^j c_j \varrho^{e_j(1)}(t) + c_j \varrho_0^j \left(\frac{c_j}{\varepsilon_j} t \right) + q_0^j \left(\frac{c_j}{\varepsilon_j} t \right), \\ \varrho^j(t, L_j) &= \alpha_1^j \varrho^{e_j(2)}(t), \quad q^j(t, L_j) = \alpha_1^j c_j \varrho^{e_j(2)}(t) - c_j \varrho_0^j \left(L_j - \frac{c_j}{\varepsilon_j} t \right) + q_0^j \left(L_j - \frac{c_j}{\varepsilon_j} t \right). \end{aligned}$$

Substituting the coupling conditions stated in (16), one can indeed show that, with these definitions,

$$\lim_{t \searrow 0} \varrho^j(t, x) = \varrho_0^j(x) \quad \text{and} \quad \lim_{t \searrow 0} q^j(t, x) = q_0^j(x) \quad \text{for } x \in \{0, L_j\}.$$

We skip these calculations here for brevity. Next, set

$$\begin{bmatrix} \varrho^j \\ q^j \end{bmatrix} (t, x) = \frac{1}{2} \begin{bmatrix} 1 & \frac{\varepsilon_j}{c_j} \\ \frac{c_j}{\varepsilon_j} & 1 \end{bmatrix} \begin{bmatrix} \varrho_*^j \\ q_*^j \end{bmatrix} \left(\frac{c_j}{\varepsilon_j} t, x \right) + \frac{1}{2} \begin{bmatrix} 1 & -\frac{\varepsilon_j}{c_j} \\ -\frac{c_j}{\varepsilon_j} & 1 \end{bmatrix} \begin{bmatrix} \varrho_*^j \\ q_*^j \end{bmatrix} \left(-\frac{c_j}{\varepsilon_j} t, x \right)$$

for $(t, x) \in (0, T] \times (0, L_j)$, where

$$\begin{bmatrix} \varrho_*^j \\ q_*^j \end{bmatrix} (t, x) = \begin{cases} \begin{bmatrix} \varrho_0^j \\ q_0^j \end{bmatrix} (x - t), & \text{if } x - t \in [0, L_j], \\ \begin{bmatrix} \varrho^j \\ q^j \end{bmatrix} \left(\frac{\varepsilon_j(t-x)}{c_j}, 0 \right), & \text{if } x - t < 0, \\ \begin{bmatrix} \varrho^j \\ q^j \end{bmatrix} \left(\frac{\varepsilon_j(-t-(L_j-x))}{c_j}, L_j \right), & \text{if } x - t > L_j. \end{cases}$$

The above considerations show that (ϱ_*^j, q_*^j) is continuous and piecewise absolutely continuous, thus absolutely continuous everywhere. To see that these functions in fact solve system (18), first note that the initial condition and the coupling condition (13) are satisfied by construction.

Moreover, for each $v \in V$ we have

$$\begin{aligned}
& \sum_{e_j \in \delta^+ v} q^j(t, L_j) - \sum_{e_j \in \delta^- v} q^j(t, 0) \\
&= \sum_{e_j \in \delta^+ v} \left[\alpha_1^j c_j \varrho_{e_j(2)}(t) - c_j \varrho_0^j \left(L_j - \frac{c_j}{\varepsilon_j} t \right) + q_0^j \left(L_j - \frac{c_j}{\varepsilon_j} t \right) \right] \\
&\quad - \sum_{e_j \in \delta^- v} \left[-\alpha_0^j c_j \varrho_{e_j(1)}(t) + c_j \varrho_0^j \left(\frac{c_j}{\varepsilon_j} t \right) + q_0^j \left(\frac{c_j}{\varepsilon_j} t \right) \right] \\
&= \left(\sum_{e_j \in \delta^+ v} \alpha_1^j c_j + \sum_{e_j \in \delta^- v} \alpha_0^j c_j \right) \varrho^v(t) \\
&\quad - \sum_{e_j \in \delta^+ v} \left[c_j \varrho_0^j \left(L_j - \frac{c_j}{\varepsilon_j} t \right) - q_0^j \left(L_j - \frac{c_j}{\varepsilon_j} t \right) \right] - \sum_{e_j \in \delta^- v} \left[c_j \varrho_0^j \left(\frac{c_j}{\varepsilon_j} t \right) + q_0^j \left(\frac{c_j}{\varepsilon_j} t \right) \right] \\
&= \alpha_v \varrho^v(t) - (\alpha_v \varrho^v(t) - q^v(t)) \\
&= q^v(t)
\end{aligned}$$

Observe that ϱ^j and q^j are continuous at the boundaries $x = 0$ and $x = L_j$ and that

$$\begin{aligned}
& A^j \frac{\partial}{\partial x} \begin{bmatrix} \varrho^j \\ q^j \end{bmatrix} (t, x) \\
&= \frac{1}{2} A^j \begin{bmatrix} 1 & \frac{\varepsilon_j}{c_j} \\ \frac{c_j}{\varepsilon_j} & 1 \end{bmatrix} \frac{\partial}{\partial x} \begin{bmatrix} \varrho_*^j \\ q_*^j \end{bmatrix} \left(\frac{c_j}{\varepsilon_j} t, x \right) + \frac{1}{2} A^j \begin{bmatrix} 1 & -\frac{\varepsilon_j}{c_j} \\ -\frac{c_j}{\varepsilon_j} & 1 \end{bmatrix} \frac{\partial}{\partial x} \begin{bmatrix} \varrho_*^j \\ q_*^j \end{bmatrix} \left(-\frac{c_j}{\varepsilon_j} t, x \right) \\
&= -\frac{\varepsilon_j}{2c_j} \begin{bmatrix} \frac{c_j}{\varepsilon_j} & 1 \\ \frac{c_j}{\varepsilon_j} & \frac{c_j}{\varepsilon_j} \end{bmatrix} \frac{\partial}{\partial t} \begin{bmatrix} \varrho_*^j \\ q_*^j \end{bmatrix} \left(\frac{c_j}{\varepsilon_j} t, x \right) + \frac{\varepsilon_j}{2c_j} \begin{bmatrix} -\frac{c_j}{\varepsilon_j} & 1 \\ \frac{c_j}{\varepsilon_j} & -\frac{c_j}{\varepsilon_j} \end{bmatrix} \frac{\partial}{\partial t} \begin{bmatrix} \varrho_*^j \\ q_*^j \end{bmatrix} \left(-\frac{c_j}{\varepsilon_j} t, x \right) \\
&= -\frac{\partial}{\partial t} \begin{bmatrix} \varrho^j \\ q^j \end{bmatrix} (t, x)
\end{aligned}$$

for a.e. $(t, x) \in (0, T] \times (0, L_j)$, thus the above construction indeed yields a solution to (18) for $T \leq \bar{T}$ with $z(t) \in D$ for $t \in [0, T]$. For the case $T > \bar{T}$ note that the same steps can be repeated successively to expand the solution for the times $[\bar{T}, 2\bar{T}]$, $[2\bar{T}, 3\bar{T}]$ and so on. To prove uniqueness of the solution, consider the case $z_0 = 0$ of initial data and introduce the energy

$$E(t) = \frac{1}{2} \sum_{e_j \in E} \int_0^{L_j} (\varrho^j(t, x))^2 + \frac{1}{c_j^2} (q^j(t, x))^2 dx.$$

Obviously, we have $E(t) = 0 \iff \varrho^j(t, \cdot) = q^j(t, \cdot) = 0 \quad \forall j = 1, \dots, n$, $E(t) \geq 0$ for all $t \geq 0$ and $E(0) = 0$. Furthermore,

$$\begin{aligned}
\frac{d}{dt}E(t) &= \sum_{e_j \in E} \int_0^{L_j} \varrho^j(t, x) \frac{\partial}{\partial t} \varrho^j(t, x) + \frac{1}{c_j^2} q^j(t, x) \frac{\partial}{\partial t} q^j(t, x) dx \\
&= \sum_{e_j \in E} \frac{1}{\varepsilon_j} \int_0^{L_j} -\varrho^j(t, x) \frac{\partial}{\partial x} q^j(t, x) + q^j(t, x) \frac{\partial}{\partial x} \varrho^j(t, x) dx \\
&\stackrel{\text{P.I.}}{=} \sum_{e_j \in E} \frac{1}{\varepsilon_j} [q^j(t, L_j) \varrho^j(t, L_j) - q^j(t, 0) \varrho^j(t, 0)] \\
&= \sum_{v \in V} \left[\sum_{e_j \in \delta^+ v} \frac{1}{\varepsilon_j} q^j(t, L_j) \varrho^j(t, L_j) - \sum_{e_j \in \delta^- v} \frac{1}{\varepsilon_j} q^j(t, 0) \varrho^j(t, 0) \right] \\
&= \sum_{v \in V} \varrho^v(t) \left[\sum_{e_j \in \delta^+ v} \frac{\alpha_1^j}{\varepsilon_j} q^j(t, L_j) - \sum_{e_j \in \delta^- v} \frac{\alpha_0^j}{\varepsilon_j} q^j(t, 0) \right] \\
&= 0,
\end{aligned}$$

since $\varrho^v \equiv 0$ for all $v \in V$. But then $E \equiv 0$, hence $z \equiv 0$. This concludes the proof for the semigroup property. \square

We now can apply standard arguments from semigroup theory for further discussion of (17): by [28, Chapter 6, Theorem 1.2 and 1.5], if the inhomogeneity f is continuously differentiable and globally Lipschitz-continuous, (17) has a unique classical solution z . Though these assumptions do not apply to the friction term f stated in (6), we can use the following technical consideration to still get a unique solution: choose any $\bar{\varrho}, \bar{q} > 0$ and define the modified right-hand side

$$\tilde{f}(z) = \begin{bmatrix} 0 \\ -\theta \frac{\min\{z_2 | z_2 |, \bar{q}\}}{\max\{z_1, \bar{\varrho}\}} - gh'z_1 \end{bmatrix}.$$

The function \tilde{f} is continuously differentiable and globally Lipschitz-continuous as a function mapping $L^2([0, L], \mathbb{R})$ onto itself for any $L > 0$. If we replace f by the \tilde{f} in (7), we then have a system fitting the assumptions made above for each fixed $k = 1, \dots, N$ and thus we have a unique solution. If we choose $\bar{\varrho}$ sufficiently small and \bar{q} sufficiently large, then the numerical simulation with realistic data shows that both the boundaries $\bar{\varrho}$ and \bar{q} will in fact never be reached by ϱ and q , respectively. In this case, however, the solution coincides with the unique solution to the original problem (7).

4. OPTIMALITY CONDITIONS AND A SOLUTION METHOD

By the results developed in Section 3, we find that the optimization problem (11) is of the form

$$\begin{aligned}
(19) \quad & \min_{\mu, \tau} J(\mu, \tau, z) \\
& \text{s.t.} \quad \dot{z}(t) = A^{\mu_k} z(t) + f^{\mu_k}(t, z(t)), \quad k \in \{1, \dots, N\}, t \in (\tau_{k-1}, \tau_k), \\
& \quad \quad z(\tau_k) = g^{\mu_k, \mu_{k+1}}(z^-(\tau_k)), \quad k \in \{1, \dots, N\}, \\
& \quad \quad z(\tau_0) = z_0, \\
& \quad \quad \tau \in \mathcal{T}(0, T).
\end{aligned}$$

where A^{μ_k} is a strongly continuous semigroup, f^{μ_k} is a semilinear perturbation and $g^{\mu_k \cdot \mu_{k+1}} = \text{id}$ is a transition map that can be chosen trivially here for each $k = 1, \dots, N$. The ordering cone $\mathcal{T}(0, T)$ is for fixed $T > 0$ defined by

$$\mathcal{T}(0, T) = \{\tau = (\tau_1, \dots, \tau_N) \in \mathbb{R}^N \mid 0 = \tau_0 \leq \tau_1 \leq \dots \leq \tau_N \leq \tau_{N+1} = T\}.$$

We summarize some results from the preliminary work in [30] on system (19) in the following: by Theorem 3.1 and the subsequent remarks, [30, Lemma 2] can be applied, yielding a control-to-state-map $(\mu, \tau) \mapsto z(\mu, \tau)$ that can be substituted into J to define the reduced cost functional $\Phi(\mu, \tau) = J(\mu, \tau, z(\mu, \tau))$. We can now apply [30, Theorem 8] to show that Φ is continuously differentiable with respect to the switching time τ_k . Recalling the shortened notation introduced in (10), we find that, while J_2 can be differentiated directly with respect to (μ, τ) , the term J_1 depends on the solution $z = z(\mu, \tau)$. Again by [30, Theorem 8], we can state gradient formulae for the derivatives of J_1 based on the *adjoint equation*

$$(20) \quad \dot{p}(t) + \begin{bmatrix} A & 0 \\ 0 & B \end{bmatrix}^* p(t) = -[f_z(z(t))]^* p(t) + l_z(z(t)), \quad t \in [0, T],$$

$$p(T) = 0.$$

Here, $f_z: Z \rightarrow L(Z)$ and $l_z: Z \rightarrow Z^*$ denote the derivatives of the friction term f and l as in (10) with respect to z . Substituting the definitions made in (15) yields that in fact $p = (p^1, \dots, p^n)$ again can be partitioned into edgewise defined functions $p^j = (p_1^j, p_2^j)^\top$ for $j = 1, \dots, n$ satisfying

$$(21) \quad \begin{bmatrix} p_1^j \\ p_2^j \end{bmatrix}_t + \begin{bmatrix} 0 & c_j^2 \\ 1 & 0 \end{bmatrix} \begin{bmatrix} p_1^j \\ p_2^j \end{bmatrix}_x = \theta \begin{bmatrix} 0 & -\frac{q^j |q^j|}{\varrho^j |q^j|} \\ 0 & 2 \frac{|q^j|}{\varrho^j} \end{bmatrix} \begin{bmatrix} p_1^j \\ p_2^j \end{bmatrix} + \gamma_1 \begin{bmatrix} \varrho^j - \varrho_d^j \\ q^j - q_d^j \end{bmatrix}$$

$$\begin{bmatrix} p_1^j \\ p_2^j \end{bmatrix} (T, x) = 0$$

as well as the coupling conditions

$$(22) \quad \alpha_{x(v, e_k)}^j p_1^j(t, L_k x(v, e_k)) = \alpha_{x(v, e_l)}^k p_1^k(t, L_l x(v, e_l)), \quad \forall e_k, e_l \in \delta v,$$

$$(23) \quad \sum_{e_j \in \delta^+ v} p_2^j(t, L_j) - \sum_{e_j \in \delta^- v} p_2^j(t, 0) = 0.$$

By [30, Lemma 6], system (20) (and thus (21),(22),(23) as well) have a unique mild solution and, applying [30, Theorem 8], the *switching time gradient* is given by

$$(24) \quad \frac{\partial \Phi}{\partial \tau_k} = \sum_{e_j \in E} \left[\int_0^{L_j} p^j(\tau_k, x) [(A^{\mu_k})^j - (A^{\mu_{k-1}})^j] z^j(\tau_k, x) dx \right. \\ \left. + \gamma_2 [(\mu_k(m) - \bar{\varepsilon})^2 - (\mu_{k-1}(m) - \bar{\varepsilon})^2] \right].$$

If the mode sequence μ is fixed, we can conclude that a switching sequence $\tau = (\tau_k)_{k=0, \dots, N+1}$ is a KKT-point of the minimization problem (11), if the following holds: For $n \in \{1, \dots, N\}$ set $a(\tau, n) = \min\{m \in \{0, \dots, n\} \mid \tau_m = \tau_n\}$ and $b(\tau, n) = \max\{m \in \{n, \dots, N+1\} \mid \tau_m = \tau_n\}$, then

$$(25) \quad \sum_{j=a(\tau, n)}^n \frac{\partial \Phi}{\partial \tau_j}(\tau) \leq 0 \quad \text{and} \quad \sum_{j=n}^{b(\tau, n)} \frac{\partial \Phi}{\partial \tau_j}(\tau) \geq 0.$$

Similarly, by [30, Theorem 10], the sensitivity of the cost function with respect to introducing a new mode μ' on an infinitesimal time interval at the point τ' can be represented by the *mode*

insertion gradient given by

$$(26) \quad \frac{\partial \Phi}{\partial \mu'}(\tau') = \sum_{e_j \in E} \left[\int_0^{L_j} p^j(\tau', x) \left[(A^{\mu_k})^j - (A^{\mu'})^j \right] z^j(\tau', x) dx \right. \\ \left. + \gamma_2 \left[(\mu_k(m) - \bar{\varepsilon})^2 - (\mu'(m) - \bar{\varepsilon})^2 \right] \right],$$

where μ_k is the original mode at time τ' . In summary, a switching sequence (μ, τ) is called *stationary*, if τ is a KKT-point for μ fixed and if $\frac{\partial \Phi}{\partial \mu'}(\tau') \geq 0$ for all modes μ' and all times $\tau' \in [0, T]$. Any global minimum of the problem (11) then is stationary.

In order to compute such stationary switching signals, we consider a conceptual algorithm originally proposed for optimal mode scheduling in hybrid ODE-dynamical systems [2]. The main idea is a two phase approach as follows: the algorithm is initialized with a switching sequence (μ^0, τ^0) , for instance $\mu^0 = 1$ and $\tau^0 = (0, T)$ where no switching occurs and the system is solved by keeping the mode constant at 1.

In a first phase, the position of available switching time points are optimized while conserving their order by using a projected-gradient method with Armijo step size. To this end a projection P onto the ordering cone $\mathcal{T}(0, T)$ is used. In a second phase, a new mode μ' is inserted at a time point τ' where $\frac{\partial \Phi}{\partial \mu'}(\tau') < 0$. If no such point exists, the switching sequence is stationary in the above sense, otherwise the algorithm continues with the first phase again.

A more precise description of the procedure is given in Algorithm 1. A convergence analysis

Algorithm 1 Two-phase gradient decent for stationary switching sequences

Require: Initial switching sequence (μ^0, τ^0) with N modes, Armijo-parameters $\beta \in (0, 1)$ and

$\gamma \in (0, 1)$

1: Set $k = 0$.

2: Solve (17) for z and (21) for p .

3: Calculate the switching time gradient $\frac{\partial \Phi}{\partial \tau^k} = \left(\frac{\partial \Phi}{\partial \tau_n^k} \right)_{n=1, \dots, N-1}$ in (24).

4: **while** τ^k does not satisfy (25) **do**

5: Find a step size $s_k = \max\{\beta^l \mid l = 0, 1, 2, \dots\}$ such that

$$\Phi \left(P \left(\tau^k - s^k \frac{\partial \Phi}{\partial \tau^k} \right) \right) \leq \Phi(\tau^k) - \gamma \frac{\partial \Phi}{\partial \tau^k}^\top \left[\tau^k - P \left(\tau^k - s^k \frac{\partial \Phi}{\partial \tau^k} \right) \right]$$

6: Set $\tau^k \leftarrow P \left(\tau^k - s^k \frac{\partial \Phi}{\partial \tau^k} \right)$.

7: Solve (7) for z and (21) for p .

8: Calculate the switching time gradient $\frac{\partial \Phi}{\partial \tau^k} = \left(\frac{\partial \Phi}{\partial \tau_n^k} \right)_{n=1, \dots, N-1}$ in (24).

9: **end while**

10: **if** the mode insertion gradient $\frac{\partial \Phi}{\partial \mu'}(\tau') \geq 0$ in (26) for all modes μ' and all $\tau' \in [0, T]$ **then**

11: **return** $(\mu, \tau) = (\mu^k, \tau^k)$

12: **end if**

13: Find mode μ' and $\tau' \in [0, T]$ with $\frac{\partial \Phi}{\partial \mu'}(\tau') < 0$ in (26).

14: Find $n \in \{0, \dots, N\}$ such that $\tau' \in [\tilde{\tau}_n^k, \tilde{\tau}_{n+1}^k)$.

15: Set $\mu^{k+1} \leftarrow (\mu_1^k, \dots, \mu_n^k, \mu', \mu_{n+1}^k, \dots, \mu_N^k)$

16: Set $\tau^{k+1} \leftarrow (\tau_1^k, \dots, \tau_n^k, \tau', \tau', \tau_{n+1}^k, \dots, \tau_N^k)$

17: Set $k \leftarrow k + 1$, $N \leftarrow N + 1$.

18: Go to 2.

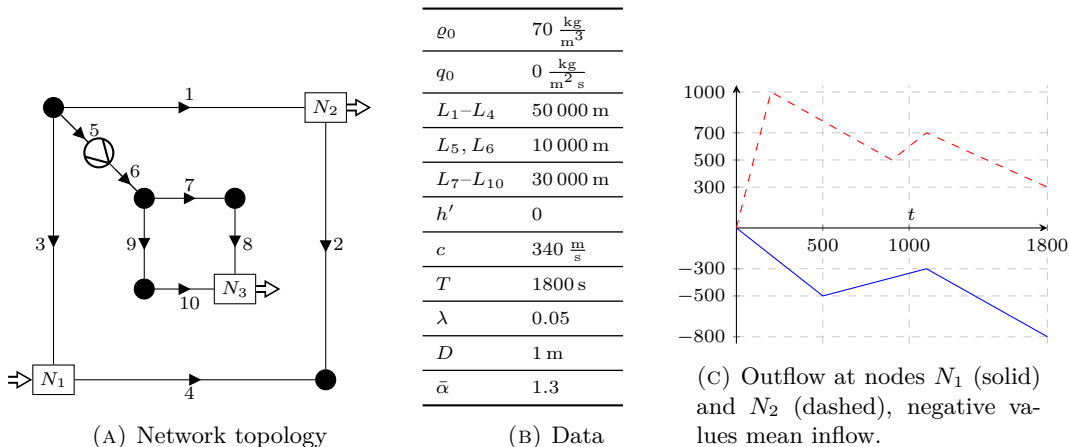


FIGURE 1. A gas network with a supply node N_1 and two customer nodes N_2 and N_3 .

for this algorithm can be found in [2]. A possible implementation of the projection P can be found in [13].

5. NUMERICAL STUDY

As a proof of concept we consider a gas network outlined in Figure 1a. At the boundary node N_1 gas is supplied to the network whereas nodes N_2 and N_3 are customer nodes where gas can possibly be taken out of the network. This can be seen as a simplified example of a big regional gas pipeline network with a local distribution subnetwork. In the particular scenario we are looking at, there is gas transported from the supply N_1 to node N_2 to satisfy a given demand while N_3 is inactive. All pipes are assumed to be horizontal ($h' = 0$), the compressor is assumed to be running at a constant compression factor $\bar{\alpha}$, compare (5), and at initial time the network is assumed to be stationary with constant densities ϱ_0 on the outer circle (thus $\alpha\varrho_0$ on the inner circle) and flux q_0 everywhere, moreover the outflows at the nodes N_1 and N_2 are outlined in Figure 1c. See the table in Figure 1b for specific values for those and other constants.

Due to the almost decoupled inner and outer circle, it can be expected that the numerical solution highly varies on the outer circle connecting N_1 and N_2 but is near to constant on the inner circle. This is confirmed by the simulation of the full model, see Figure 2 for a snapshot of the simulation at the time $t = 900$ s. We therefore can suspect that the simulation on the inner circle can be widely frozen with only some small losses in the accuracy of the solution. Indeed, letting \bar{z} be the distinguished solution to (7),(8) resulting from freezing the solution completely on the inner edges 6 to 10, our simulations show that the L^2 -errors of the density and the flux relative to the respective maximum values in z_d is less than 1% for ϱ and less than 6.5% for q ; see Figure 3a. Moreover, compared to a full simulation z_d about half of the computation time in the sense of J_2 defined in (10) is saved.

In our implementation the system (7),(8) is solved via splitting of the hyperbolic part and the friction term. For the simulation of the hyperbolic part we use the *2-step-Richtmyer-method with artificial viscosity* that, given a system matrix A and a discretization $z^k = (z_1^k, \dots, z_n^k)^\top$ with spatial step size Δx of the solution at time point t_k , computes the discretized values z^{k+1}

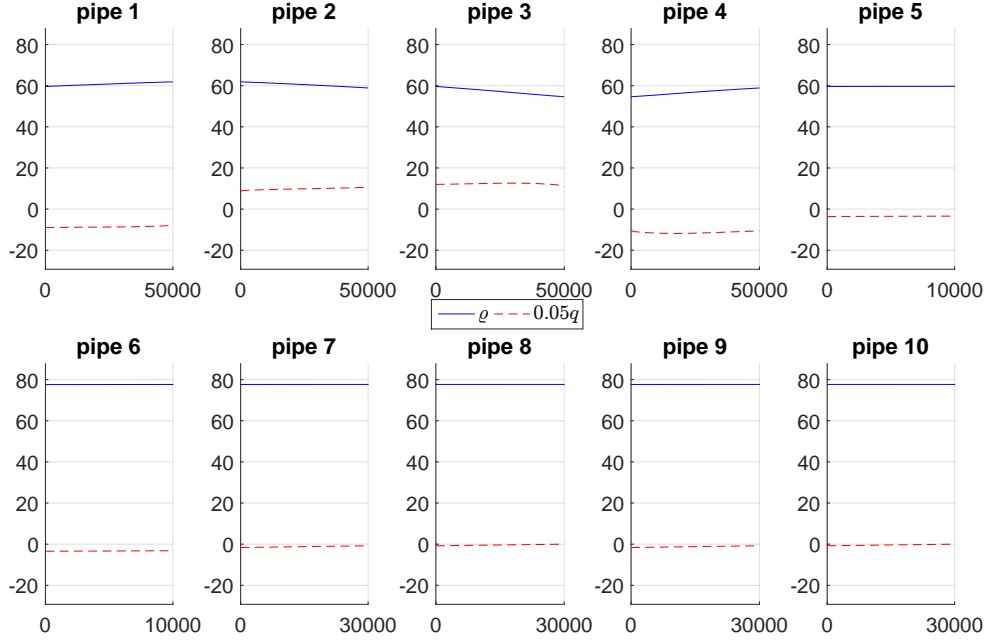


FIGURE 2. Snapshot of the fully simulated solution showing density (solid, blue) and flux (dashed, red, scaled by 0.05). On the outer pipes 1 to 5 we see a lot of fluctuation due to the oscillatory boundary flows. The pipes 6 to 9 of the inner circle, however, remain nearly constant.

at time $t_{k+1} = t_k + \Delta t$ by the explicit finite-volume-scheme

$$z_{j+\frac{1}{2}}^{k+\frac{1}{2}} = \frac{1}{2} (z_{j+1}^k + z_j^k) - \frac{\Delta t}{2\Delta x} A (z_{j+1}^k - z_j^k),$$

$$z_j^{k+1} = z_j^k - \frac{\Delta t}{\Delta x} A \left(z_{j+\frac{1}{2}}^{k+\frac{1}{2}} - z_{j-\frac{1}{2}}^{k+\frac{1}{2}} \right) + \varepsilon (z_{j+1}^k - 2z_j^k + z_{j-1}^k)$$

for $j = 1, \dots, n$, where $\varepsilon \sim 0.05$ introduces an additional, minor but stabilizing smoothing to the solution, see [21, Chapter 18.1]. The discretization is chosen in a way such that the cells z_1^k and z_n^k are centered at the boundary points $x = 0$ and $x = 1$, respectively. The time step is done for the solution on each single pipe after appropriate ghost cell values $(z^e)_0^k, (z^e)_{n+1}^k$ for each $e \in E$ are derived from the coupling conditions. We mention without further proof that these can be solved explicitly for each node $v \in V$ by first setting the weighted mean value

$$z_*^v = \frac{2}{|\delta v|} \left(\sum_{e \in \delta^+ v} (z^e)_{n-1}^k + \begin{bmatrix} 1 & 0 \\ 0 & -1 \end{bmatrix} \sum_{e \in \delta^- v} (z^e)_2^k \right)$$

and then using the ghost cell values

$$\begin{aligned} (z^e)_{n+1}^k &= \begin{bmatrix} 1 & 0 \\ 0 & -1 \end{bmatrix} (z_*^v - (z^e)_{n-1}^k) & \text{for all } e \in \delta^+v, \\ (z^e)_0^k &= z_*^v - \begin{bmatrix} 1 & 0 \\ 0 & -1 \end{bmatrix} (z^e)_2^k & \text{for all } e \in \delta^-v. \end{aligned}$$

Here, in each time step, we incorporate only those edges where the solution is actively calculated. In the special case if $v \in V$ is a compressor, we only have one ingoing edge $e_+ \in \delta^+v$ and one outgoing edge $e_- \in \delta^-v$ and instead have to set

$$\begin{aligned} z_*^v &= \frac{2}{1 + \bar{\alpha}} \left((z^{e_+})_{n-1}^k + \begin{bmatrix} 1 & 0 \\ 0 & -1 \end{bmatrix} (z^{e_-})_2^k \right), \\ (z^{e_+})_{n+1}^k &= \begin{bmatrix} 1 & 0 \\ 0 & -1 \end{bmatrix} (z_*^v - (z^{e_+})_{n-1}^k), \\ (z^{e_-})_0^k &= \begin{bmatrix} \bar{\alpha} & 0 \\ 0 & 1 \end{bmatrix} z_*^v - \begin{bmatrix} 1 & 0 \\ 0 & -1 \end{bmatrix} (z^{e_-})_2^k. \end{aligned}$$

For the friction term, we add an explicit Runge-Kutta-step using the classical *Runge-Kutta-scheme of order 4*. The same methods are used on the same discretization grid backwards in time to solve the adjoint system stated in (21),(22),(22). To evaluate the gradient formulae (24) and (26), we use the trapezoidal rule over the spatial grid. The expression $[(A^{\mu_k})^j - (A^{\mu_{k-1}})^j]z^j(\tau_k, x)$ occurring in both (24) and (26) represents the difference of the time derivatives of the solution depending on which mode μ_k is switched to. In the numerical scheme, this is realized by calculating a time step of the solution for each choice of μ_k and then subtracting the forward difference quotients.

The fixed temporal discretization grid for the actual solution is supplemented by a grid of switching time points that may vary due to the superordinated optimization where the data needed for the gradient formulae is calculated. For our study we start the optimization with the fully frozen solution, where in no time step the model (2) is actually calculated, and iteratively insert regions of active numerical solving wherever the gradients indicate a major loss of accuracy. Applying the projected-gradient method with sequential mode insertion described in Algorithm 1 yields the results shown in Figure 3b. We observe that it is in fact almost unnecessary to calculate the fine model on the edges 6 to 10 of the inner circle and that the algorithm indeed approximates the distinguished solution \bar{z} as expected. However, since Algorithm 1 does not remove switching points, there remain scattered short intervals where the mode is switched twice almost instantly. These switching points can be removed from the solution by applying a posteriori filtering.

6. CONCLUSION

We have presented an application of the theory of switching systems to a model hierarchy for the dynamics of gas in a pipeline network. A semigroup formulation was given for the model on gas networks including time-dependent outflow at each node as well as a linearized model for compressors that allowed us to prove the existence of unique solutions. Using adjoint-based gradient representations for switching abstract evolution systems, we implemented a two stage projected-gradient descent method for the optimization of switching between different levels of accuracy in the hierarchy. As an example, we optimized the simulation of a small supply network by freezing the calculation on edges whenever the numerical error made is small compared to the computational costs.

Our prototypical approach can be applied in a similar fashion to realistic industrial networks. The technique can also be extended to identify a model switching strategy for a reduced model

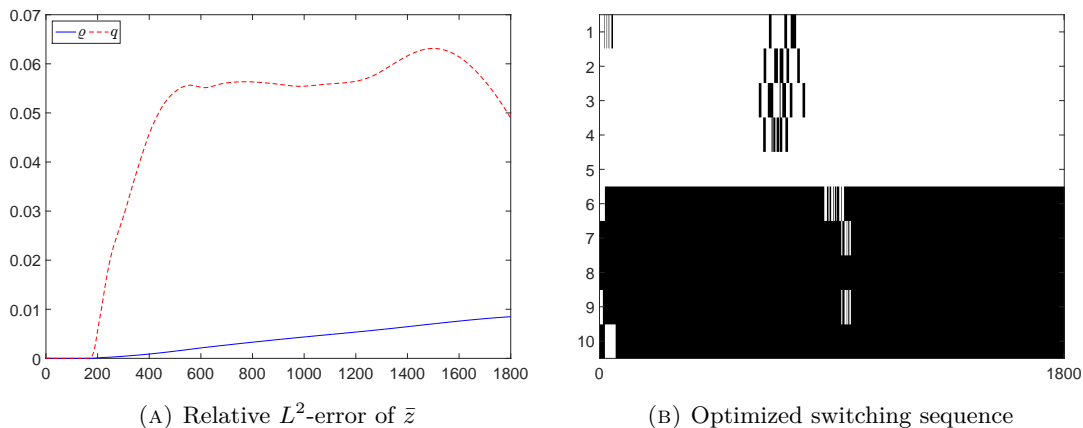


FIGURE 3. left: L^2 -error relative to maximum values of the solution \bar{z} corresponding to freezing edges 6 to 10 completely; right: resulting optimized switching sequence showing, for each time step from $t_0 = 0$ s to $T = 1800$ s and each edge e_1, \dots, e_{10} , if the solution is calculated with the fine model (white) or frozen (black).

using a range of different parameter configurations such as representing different boundary flow scenarios, compressor settings and valve positions. The resulting reduced simulation model can then be used for a time expanded mixed-integer optimization technique based on full discretization with a minimum of variables or within a bilevel optimisation method which optimises a cost functional on the outer level with optimal efficiency on the lower level as proposed, for example, in [16]. Further directions include a combination of this method in a network of submodel hierarchies such as those used in [26] for the optimisation of stationary models.

ACKNOWLEDGEMENTS

The authors thank the Deutsche Forschungsgemeinschaft for their support within the projects A03 and B03 in the Sonderforschungsbereich/Transregio 154 *Mathematical Modelling, Simulation and Optimization using the Example of Gas Networks*.

REFERENCES

- [1] M. A. Adewumi and J. Zhou. *Simulation of Transient Flow in Natural Gas Pipelines*. 27th Annual Meeting of PSIG (Pipeline Simulation Interest Group), Albuquerque, NM. 1995.
- [2] H. Axelsson et al. “Gradient descent approach to optimal mode scheduling in hybrid dynamical systems”. In: *J. Optim. Theory Appl.* 136.2 (2008), pp. 167–186. DOI: 10.1007/s10957-007-9305-y.
- [3] M. K. Banda, M. Herty, and A. Klar. “Gas flow in pipeline networks”. In: *Netw. Heterog. Media* 1.1 (2006), pp. 41–56.
- [4] B. Baumrucker, J. Renfro, and L. T. Biegler. “MPEC problem formulations and solution strategies with chemical engineering applications”. In: *Computers & Chemical Engineering* 32.12 (2008), pp. 2903–2913.
- [5] L. Biegler. *Nonlinear Programming: Concepts, Algorithms, and Applications to Chemical Processes*. Philadelphia, PA.: SIAM, 2010.

- [6] J. Brouwer, I. Gasser, and M. Herty. “Gas Pipeline Models Revisited: Model Hierarchies, Nonisothermal Models, and Simulations of Networks”. In: *Multiscale Modeling & Simulation* 9.2 (2011), pp. 601–623. DOI: 10.1137/100813580. eprint: <http://epubs.siam.org/doi/pdf/10.1137/100813580>.
- [7] J. Brouwer, I. Gasser, and M. Herty. “Gas pipeline models revisited: model hierarchies, nonisothermal models, and simulations of networks”. In: *Multiscale Model. Simul.* 9.2 (2011), pp. 601–623. DOI: 10.1137/100813580.
- [8] C. G. Cassandras, D. L. Pepyne, and Y. Wardi. “Optimal Control of a Class of Hybrid Systems”. In: *IEEE Trans. Automat. Control* 46.3 (2001), pp. 398–415.
- [9] M. Dick, M. Gugat, and G. Leugering. “Classical solutions and feedback stabilization for the gas flow in a sequence of pipes”. In: *Netw. Heterog. Media* 5.4 (2010), pp. 691–709. DOI: 10.3934/nhm.2010.5.691.
- [10] P. Domschke et al. *Adaptive Refinement Strategies for the Simulation of Gas Flow in Networks using a Model Hierarchy*. Tech. rep. 2017/03. arxiv: <http://arxiv.org/abs/1701.09031>. TU Berlin, Institute for Mathematics, 2017.
- [11] P. Domschke, O. Kolb, and J. Lang. “Adjoint-based error control for the simulation and optimization of gas and water supply networks”. In: *Appl. Math. Comput.* 259 (2015), pp. 1003–1018. DOI: 10.1016/j.amc.2015.03.029.
- [12] P. Domschke et al. *Modellierung von Gasnetzwerken: Eine Übersicht*. Technische Universität Darmstadt, 2017, p. 33.
- [13] M. Egerstedt, Y. Wardi, and H. Axelsson. “Transition-time Optimization for Switched-Mode Dynamical Systems”. In: *Automatic Control, IEEE Transactions on* 51.1 (2006), pp. 110–115.
- [14] M. Gugat et al. “Stationary states in gas networks”. In: *Netw. Heterog. Media* 10.2 (2015), pp. 295–320. DOI: 10.3934/nhm.2015.10.295.
- [15] M. Hahn, S. Leyffer, and V. M. Zavala. *Mixed-Integer PDE-Constrained Optimal Control of Gas Networks*. Tech. rep. Preprint ANL/MCS-P7095-0817, Argonne National Laboratory, Mathematics and Computer Science Division, 2017.
- [16] F. M. Hante et al. “Challenges in Optimal Control Problems for Gas and Fluid Flow in Networks of Pipes and Canals: From Modeling to Industrial Applications”. In: *Industrial Mathematics and Complex Systems: Emerging Mathematical Models, Methods and Algorithms*. Ed. by P. Manchanda, R. Lozi, and A. H. Siddiqi. Singapore: Springer Singapore, 2017, pp. 77–122. DOI: 10.1007/978-981-10-3758-0_5.
- [17] M. Herty and V. Sachers. “Adjoint calculus for optimization of gas networks”. In: *Netw. Heterog. Media* 2.4 (2007), pp. 733–750.
- [18] A. Heydari and S. Balakrishnan. “Optimal Switching Between Autonomous Subsystems”. In: *J. Franklin Inst.* 351.5 (2014), pp. 2675–2690.
- [19] E. R. Johnson and T. D. Murphey. “Second-Order Switching Time Optimization for Nonlinear Time-Varying Dynamic Systems”. In: *Automatic Control, IEEE Transactions on* 56.8 (2011), pp. 1953–1957.
- [20] S. L. Ke and H. C. Ti. “Transient analysis of isothermal gas flow in pipeline networks”. In: *Chem. Eng. J.* 76.2 (2000), pp. 169–177. DOI: 10.1016/S1385-8947(99)00122-9.
- [21] C. B. Laney. *Computational Gasdynamics*. Cambridge University Press, 1998.
- [22] R. J. Le Veque. *Finite Volume Methods for Hyperbolic Problems*. Cambridge University Press, 2002.
- [23] R. J. Le Veque. *Numerical Methods for Conservation Laws*. Birkhäuser, 1992.
- [24] H. W. J. Lee et al. “Control parametrization enhancing technique for optimal discrete-valued control problems”. In: *Automatica J. IFAC* 35.8 (1999), pp. 1401–1407. DOI: 10.1016/S0005-1098(99)00050-3.

- [25] D. Mahlke, A. Martin, and S. Moritz. “A mixed integer approach for time-dependent gas network optimization”. In: *Optim. Methods Softw.* 25.4-6 (2010), pp. 625–644. DOI: 10.1080/10556780903270886.
- [26] V. Mehrmann, M. Schmidt, and J. Stolwijk. *Model and Discretization Error Adaptivity within Stationary Gas Transport Optimization*. Preprint 11-2017. <http://arxiv:1712.02745>. Institute of Mathematics, TU Berlin, 2017.
- [27] V. Mehrmann and L. Wunderlich. “Hybrid systems of differential-algebraic equations - Analysis and numerical solution”. In: *J. Process Contr.* 19.8 (2009), pp. 1218–1228.
- [28] A. Pazy. *Semigroups of Linear Operators and Applications to Partial Differential Equations*. Vol. 44. Springer Science & Business Media, 2012.
- [29] M. E. Pfetsch et al. “Validation of nominations in gas network optimization: models, methods, and solutions”. In: *Optim. Methods Softw.* 30.1 (2015), pp. 15–53. DOI: 10.1080/10556788.2014.888426.
- [30] F. Rüffler and F. M. Hante. “Optimal switching for hybrid semilinear evolutions”. In: *Nonlinear Anal. Hybrid Syst.* 22 (2016), pp. 215–227. DOI: 10.1016/j.nahs.2016.05.001.
- [31] F. Rüffler and F. M. Hante. “Optimality Conditions for Switching Operator Differential Equations”. In: *Proc. Appl. Math. Mech.* To appear, 2017.
- [32] S. Sager. “Reformulations and Algorithms for the Optimization of Switching Decisions in Nonlinear Optimal Control”. In: *Journal of Process Control* 19.8 (2009), pp. 1238–1247.
- [33] J. Smoller. *Shock Waves and Reaction-Diffusion Equations*. Vol. 258. Grundlehren der mathematischen Wissenschaften. Springer, 1983.
- [34] Y. Wardi, M. Egerstedt, and M. Hale. “Switched-mode systems: gradient-descent algorithms with Armijo step sizes”. In: *Discrete Event Dyn. Syst.* 25.4 (2015), pp. 571–599. DOI: 10.1007/s10626-014-0198-2.
- [35] X. Xu and P. J. Antsaklis. “Optimal control of switched autonomous systems”. In: *Decision and Control, 2002, Proceedings of the 41st IEEE Conference on*. Vol. 4. Dec. 2002, 4401–4406 vol.4. DOI: 10.1109/CDC.2002.1185065.
- [36] X. Xu and P. J. Antsaklis. “Optimal Control of Switched Systems Based on Parameterization of the Switching Instants”. In: *IEEE Trans. Automat. Control* 49.1 (2004), pp. 2–16.
- [37] F. Zhu and P. J. Antsaklis. “Optimal control of hybrid switched systems: a brief survey”. In: *Discrete Event Dyn. Syst.* 25.3 (2015), pp. 345–364. DOI: 10.1007/s10626-014-0187-5.